ZURICH, SWITZERLAND
6 - 10 OCTOBER 2025

EUROPEAN GEOTHERMAL CONGRESS 2025

# Geochemical analyses of Triassic rocks in the Upper Rhine Graben: A first lithium study in sedimentary rocks of Soultz-sous-Forêts wells.

Carole Glaas[1], David Fries[1], Gabrielle Rumbach[1], Albert Genter[1]

[1]ES-Géothermie, 26 boulevard du Président Wilson, France

carole.glaas@es.fr

**Keywords:** Lithium, geothermal reservoir, Muschelkalk limestone, Buntsandstein sandstone, Upper Rhine Graben, rock geochemistry.

## ABSTRACT

The Upper Rhine Graben (URG) is a promising area for geothermal lithium (Li) extraction. Li concentrations in deep geothermal brine exceed 150 mg/L and are combined with significant flowrates suitable for geothermal power and heat production. However, there is still a lack of knowledge in the mechanisms leading to the brine enrichment in Li. Based on a total of 34 core samples collected from both the Triassic limestone and the sandstone from the Soultz-sous-Forêts wells (GPK-1 and EPS-1), this study aims to characterize the Li content of the samples according to depth and the lithostratigraphy. Also, this study aims to correlate the Li content with the eventual mineralogical changes underwent by the rock induced by fluid-rock interactions (precipitation and/or dissolution) in the case of diagenesis or hydrothermal circulations channelized by natural fractures.

Additionally, a comparison of Li content between Variscan and Triassic rocks allows to make the hypothesis that the water-rock interactions in both lithologies allow to put Li in solution, released from phyllosilicates. The Li in solution in the brine could then be trapped preferentially in permeable zones in all lithologies but reaching significant higher values in the deep-seated granite.

Also, as in the Muschelkalk and the Buntsandstein the Li concentration varies only between 1 and 90 ppm, compared to up to 1938 ppm in the granite, which could eventually suggest that the brine could contain more Li in solution in the Triassic formations. These results refine the story behind high Li concentration in the URG brine and eventually underlines specific reservoir zones where Li concentration could be enriched in the brine.

## 1. INTRODUCTION

The concentrations of lithium within the geothermal brines of the Upper Rhine Graben are rather documented properly and are ranging from 160 to 210 mg/L in average (Bosia et al., 2021; Sanjuan et al., 2016). However, there are only a few studies that characterize how lithium was released from geological formations to the geothermal fluids. Based on core samples collected in geothermal exploration wells at Soultz-sous-Forêts (SsF, France), a geochemical characterization of major and trace elements, including lithium, was achieved. A total of 34 rock samples, collected in the Triassic sedimentary formations from the Muschelkalk and the Buntsandstein lithostratigraphic units, was analysed and is discussed in this paper. These sedimentary rock analyses complete the dataset obtained with granite measured at different alteration stages (Fries et al., 2025). The aim of this study is to better understand the lithium enrichment in the geothermal fluids, despite the complex interactions that have occurred between Triassic sediments, the crystalline basement, and hydrothermal fluids over various locations and periods.

## 2. GEOLOGICAL SETTING

### 2.1 Geothermal site setting

The SsF site is in the URG, which is a Cenozoic rift structure showing a series of thermal anomalies characterized by a thermal gradient up to 100 °C/km (Figure 1). Those anomalies are interpreted as the trace of natural brine advection inside a nearly vertical fracture system cross-cutting both deep-seated Triassic sediments and Palaeozoic crystalline basement (Genter et al., 2010). The SsF geothermal site is located on a local horst structure bounded by normal faults showing an apparent off-set of 500 m. Deep geothermal boreholes were drilled to 5000 m depth that penetrated a sedimentary pile of 1400 m thick made of Tertiary and eroded Jurassic and Permo-Triassic sediments including Muschelkalk limestone and Buntsandstein sandstone (Figure 1). Three wells, named GPK-2, GPK-3 and GPK-4, reached 5000 m deep. Only GPK-1 (3600 m) and EPS-1 (2230 m) wells were partly to fully cored respectively in the Triassic and Palaeozoic formations and correspond to exploration wells. Therefore, the core samples used in this study come exclusively from GPK-1 and EPS-1. Today, GPK-2 is used as a production well with a flow rate of 30 kg/s at around 150 °C, while GPK-3 and GPK-4 serve as reinjection wells. The binary plant has an installed

capacity of 1.8 MWe and is operating since 2016 (Ravier et al., 2022). It is planned to drill new wells in the coming years for developing the production of the SsF site.

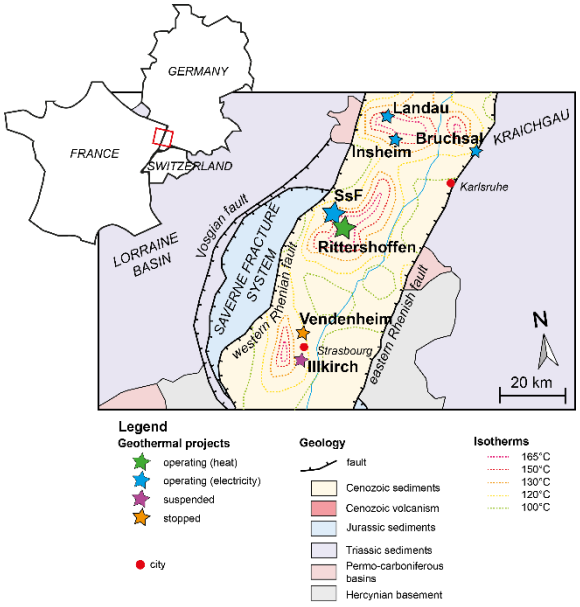


**Figure 1: Geological map of the Upper Rhine Graben centered on Soultz-sous-Forêts (SsF). Operating power plants of SsF, Rittershoffen; Bruchsal, Insheim and Landau exploit deep geothermal reservoirs discharging lithium-rich brines.**

In terms of reservoir exploitation, only the fractured granite was exploited for geothermal production at SsF. Therefore, the geothermal fluid bearing lithium is only produced from the deep fractured crystalline basement and fully reinjected at lower temperature in the same reservoir. On the contrary, in the closest Rittershoffen geothermal site, the geothermal fluid is produced from both geological formations: the Buntsandstein fractured sandstone and the deep fractured basement. An example of a steeply dipping permeable fracture is clearly visible in the production well GRT-2 (Figure 2). This natural fracture intersects its open hole section in the Buntsandstein sandstone. Thus, both the fractured sandstone and the fractured granite contributed to the fluid produced on surface.

The geochemical characterization of the geothermal brine at SsF was published by many authors (Bosia et al., 2021; Fries et al., 2025; Sanjuan et al., 2016). Geothermal water at SsF is mainly enriched in chlorine (Cl), sodium (Na), calcium (Ca) and potassium (K) with significant amount of Li which is the 5$^{th}$ most abundant element in the liquid phase with about 25 mmol/L (Fries et al., 2025). The geothermal fluid chemistry at SsF is close to other locations in the URG with a total dissolved solid around 100 g/L or more (Bruchsal, Insheim, Landau, Rittershoffen, Figure 1). suggesting that despite the slight differences in total salinity and isotopes ratios, most of the fluids have a common origin (Sanjuan et al., 2016). However, the exact contribution of flow from the fractured Triassic formations and the fractured granite remains unclear. Additionally, the impact of matrix permeability on the well flow rate is still uncertain and requires further investigation.

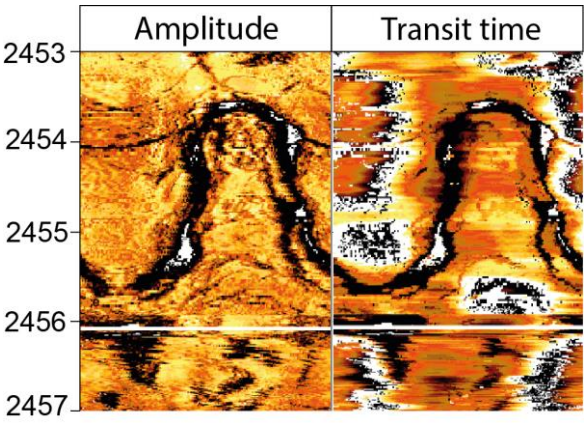


**Figure 2: Example of a permeable fracture in the GRT-2 well at Rittershoffen, visible on acoustic borehole images in amplitude and transit time and crossing the Buntsandstein sandstone.**

### 2.2 Muschelkalk limestone and Buntsandstein sandstone

The exploration well EPS-1 was cored both in the Muschelkalk limestone and the Buntsandstein sandstone but those sedimentary layers are poorly documented in terms of lithium content by comparison with the deep granite (Fries et al., 2025).

The main lithostratigraphic units were defined in this area by Aichholzer et al. (2019), based on 1 m of core in the Lettenkohle, 70 m of core in the Muschelkalk, and 410 m of core in the Buntsandstein from the SsF site. The Muschelkalk corresponds to Middle Triassic formations and represents the main marine episode in this area. It displays mainly argillaceous limestones, marl/limestone alternations, limestones, dolomites and dolomitic marls and some anhydrite (Figure 3).

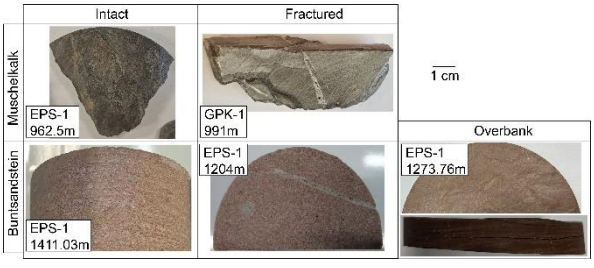


**Figure 3: Rock samples representative of the intact or fractured Muschelkalk and Buntsandstein as well as overbanks.**

The EPS-1 cores started in the Middle Muschelkalk. Occurrences of natural fractures as well as hydraulic breccias were observed in the Muschelkalk (Aichholzer et al., 2019). For example, at Rittershoffen site, the largest permeable fractured zone observed during drilling operation of the reinjection well GRT-1, was observed at the top of the Lower Muschelkalk. This permeable fractured zone is no more accessible in the

open hole section of this well which is cased (Baujard et al., 2017). The Lower Muschelkalk represents the first marine transgression covering the clastic Buntsandstein which corresponds to a vertical succession of fluvial and aeolian facies.

Those clastic formations underwent several diagenetic events: early diagenesis, burial diagenesis, and diagenesis related to hydrothermal fluid circulation in fractures (Figure 4).

Recent sedimentological studies showed that facies and facies associations control the permeability heterogeneity distribution. It turns out that fluvial channel facies association represents preferential flow units whereas wind- and water-laid facies association acts as flow barriers or baffles (Bofill et al., 2025). Moreover, compaction is considered as the primary diagenetic process affecting Lower Grès Vosgien porosity. However, geothermal reservoir quality inside the URG was poorly investigated due to a lack of well testing and geothermal production data from those limestone and clastic layers. Matrix porosity in the fluvio-aeolian deposits or the occurrence of fractured zones and/or local faults cross-cutting those clastic layers represent potential candidates for geothermal fluid migration. Based on published geothermal datasets in the URG like Rittershoffen and Bruchsal (Baujard et al., 2017; Kölbel et al., 2021), permeability is mainly controlled by fractured zones in those Permo-Triassic formations. However, hydraulic tests able to quantify the respective contribution to fluid flow of the potential URG reservoirs (Muschelkalk, Buntsandstein or Rotliegend, Carboniferous basement) are currently missing. Therefore, a better understanding of the reservoir properties (e.g. chemical composition) of the Triassic layers is needed to decipher the respective contributions of the different reservoirs. Combined with analyses of lithium content in the rocks, this will aid future lithium exploration in the URG. Detailed structural analysis of EPS-1 cores showed an average fracture density of about 0.7 fract/m in the limestone and sandstone. Locally, a cluster of natural fractures filled with secondary barite and galena depicted the trace of a local fault zone inside the sandstones at about 1200 m depth (Vernoux et al., 1995).

Based on petrographic observations of core, diagenetic processes like mineral dissolution and precipitation were described (Vernoux et al., 1995). Burial diagenesis and hydrothermal fluid circulation in fractures are mainly responsible for mineral dissolutions (feldspar, barite) and precipitations like silicification, sulphides, sulphates, and carbonates (Figure 4).

## 3. MATERIALS AND METHODS

Based on the geological heritage of the geothermal sites preserved, particularly in terms of cores, a rock sampling strategy was initiated to explore the whole geochemistry of the Triassic formations on the SsF site. Indeed, this study is the first to propose a geochemical characterization including lithium dosage of the whole depth column of Triassic formations. The objective of the sampling was to recover representative samples of the lithostratigraphy sequence of the Muschelkalk and the Buntsandstein along depth as well as representative of the tectonic and hydrothermal alteration in GPK-1 and EPS-1 wells (Figure 3 & Figure 7). This sampling was meticulously realized to ensure that each class was represented by a minimum of samples (2 or 3 preferably): 6 for the limestone, 3 for the fractured limestone, 4 for the fractured limestone with calcite, 3 for the transition between Muschelkalk and Buntsandstein, 8 for the sandstone, 5 for the fractured sandstone, and only 2 for the overbanks which are deposits formed on the flanks of fluvial channels and are mostly fine-grained and clayey.

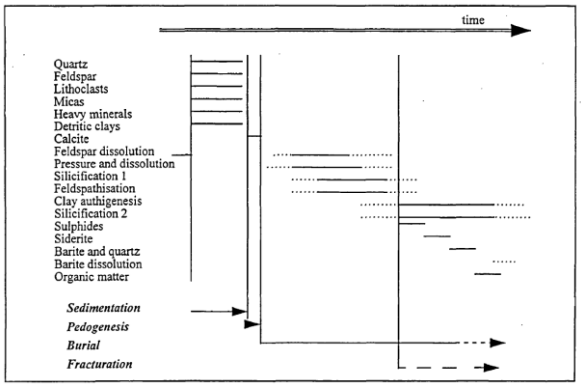


**Figure 4: Main diagenetic phases observed in the Buntsandstein sandstones (Vernoux et al., 1995).**

The geochemical analyses for the selected rock samples were carried out at the Service d'Analyse des Roches et des Minéraux (SARM) of the Centre de Recherches Pétrographiques et Géochimiques (CRPG) in Nancy, France. Before analyses, all the rock samples were grinded to reach a particle size of solid samples lesser than 80 µm. Major and minor elements ($SiO_2$, $Al_2O_3$, $Fe_2O_3$, MnO, MgO, CaO, $Na_2O$, $K_2O$, $P_2O_5$, $TiO_2$) were analysed by ICP-OES (Inductively Coupled Plasma - Optical Emission Spectrometry) ICAP 6500 following the methodology and preparation described in Carignan et al., (2001). Loss of ignition (LOI) was determined by gravimetric analyses at 1020°C. Cl analyses were performed by UV visible spectrophotometry and Li concentration were measured by flame atomic absorption spectrometry.

## 4. RESULTS & INTERPRETATION

### 4.1 Major elements and LOI

The chemical composition of major elements and LOI analyzed in the sampled sedimentary rocks are illustrated in Figure 5. Chemical variations of the different geological sedimentary formations are described separately.

- Muschelkalk formation

The Muschelkalk geological formation is primarily composed of sedimentary rocks enriched in carbonate minerals (e.g. calcite $CaCO_3$ and dolomite

($CaMg(CO_3)_2$)). As described in section 2, distinct facies were selected based on the physical characteristics of the rocks, particularly focusing on the presence or absence of natural fractures. The Muschelkalk rocks (n = 13) have a chemical composition dominated by CaO (15.2 to 40.8%) followed by $SiO_2$ (1.4 to 30.6%), MgO (0.5 to 17%), $Al_2O_3$ (0.4 to 10.0%), $Fe_2O_3$ (0.2 and 4.3%) and $K_2O$ (3.6 to 4.3%). LOI, which can be used for determining moisture and volatile materials present in the rock, ranges from 5.3 to 39.6% in Muschelkalk rocks. These high LOI values reflect the important presence of carbonates in these samples. Fractured limestone samples have a higher content of CaO and MgO compared to the non-fractured samples. When these fractured samples exhibit distinguishable veins in the rock matrix, the total amount of CaO increases further, along with the appearance of a chemical composition that was not identified during the initial analyses (Figure 5).The concentrations of Li ([Li]) range from 7 to 72 ppm in Muschelkalk rocks and are the first geochemical data of Li presented in the literature for deep sedimentary rocks at SsF (Figure 6). These values are close to previous [Li] measured in fresh monzonite granite (from 36 to 74 ppm) from the same wells (Fries et al., 2025). In these limestone rocks, [Li] are lower in the fractured limestone filled with calcite ([Li] median = 15 ppm; n = 3) compared to the rest of the limestone rocks (median = 37 ppm; n = 10). Interestingly, these [Li] are also higher than the one measured in limestones worldwide (Horstman, 1957; Weynell et al., 2017). Cl concentrations ([Cl]) measured in the Muschelkalk rocks vary from 52 to 540 ppm (Figure 6). Similar variations of [Cl] were observed in Johns and Huang, 1967 study with an average of 131 ppm in limestones and 659 ppm in dolostones. In the monzonite granite, [Cl] were averaging at 230 ppm (n = 4) and were globally lower than in the Muschelkalk samples (Fries et al., 2025).

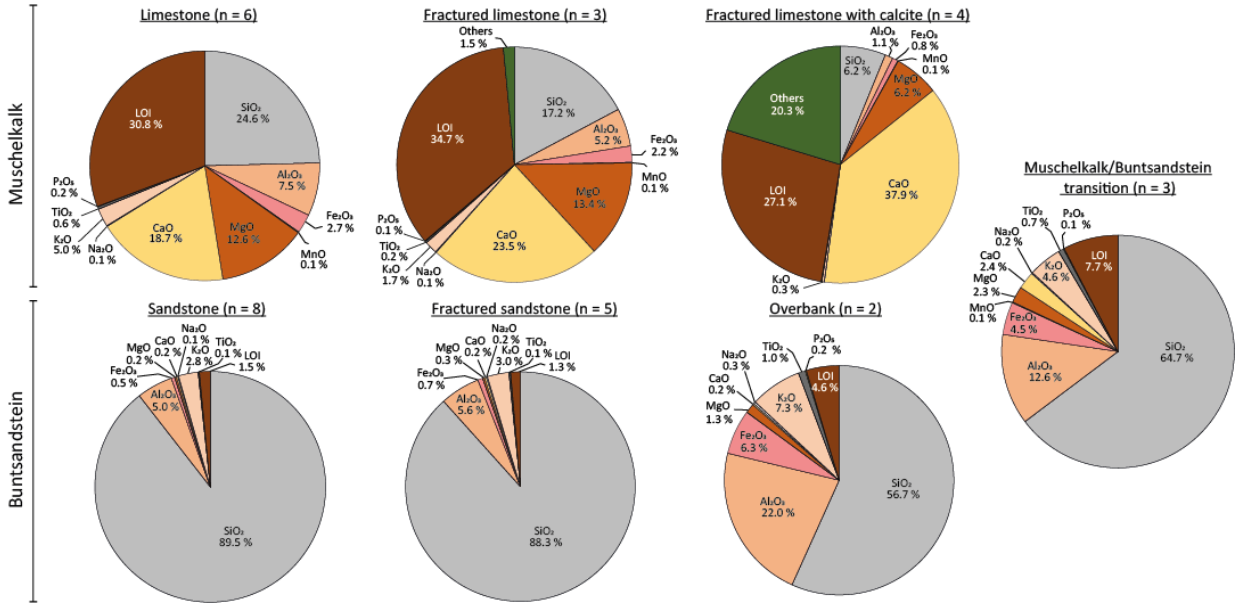


**Figure 5: Average concentration of major chemical elements measured in the different sedimentary rock sampled in the Muschelkalk and Buntsandstein geological formation. In the fractured limestone, not all elements were accounted for in the analyses and therefore are displayed as "others".**

- Buntsandstein sandstone

The Buntsandstein formation primarily consists of a 450 m thick sequence of continental red sandstone, which ranges from fine to coarse-grained and includes some conglomeratic beds. Like Muschelkalk rocks, distinct facies were selected based on the physical characteristics of the rocks. Sandstone and fractured sandstone have a very close chemical composition regarding the major elements (Figure 5). Their chemistry is highly dominated by $SiO_2$ (78.5 to 93.0%), $Al_2O_3$ (2.3 to 11.1%), $K_2O$ (1.3 to 5.1%) and $Fe_2O_3$ (0.1 to 1.1%). LOI ranges from 0.7 to 2.6% and is also similar in both fractured or not sandstone samples. Overbank samples have a distinct chemical composition in comparison to the rest of Buntsandstein rocks and have lower $SiO_2$ content and higher $Al_2O_3$, $K_2O$, LOI and $Fe_2O_3$ content (Figure 5).

The core samples collected in the Buntsandstein formation have a [Li] that ranges from 25 to 71 ppm ([Li] median = 32 ppm; Figure 6). Globally, these [Li] values are lower than [Li] measured in the fresh monzonite granite ([Li] median = 51 ppm) (Fries et al., 2025).

Buntsandstein rocks have a [Cl] comprised between 185 to 3440 ppm (Figure 6). The highest [Cl] are mainly visible in the sandstone unaffected by natural fracturing ([Cl] median = 1005 ppm). These values are the highest measured in the sampled rocks (granite rocks included). Determinations of chlorine was conducted in sandstone originating from Japan (Ogita et al., 1967), and that Cl content could vary from 10 to 1500 ppm. For these sandstones, Cl were in the form of fluid and/or soluble inclusions.

In addition to Muschelkalk and Buntsandstein core rock samples, three samples were collected at the transition between the two geological formations at 1000 - 1009 m depth. The chemical composition of these rocks resembles the composition of the overbank samples with lower $Al_2O_3$ (9.5 to 15.6%) and higher $SiO_2$ (55.2 to 70.4%). A clear influence of the Muschelkalk in the top Buntsandstein samples composition is noticeable due to the increase in the amount of CaO and MgO compared to the rest of the Buntsandstein rocks.

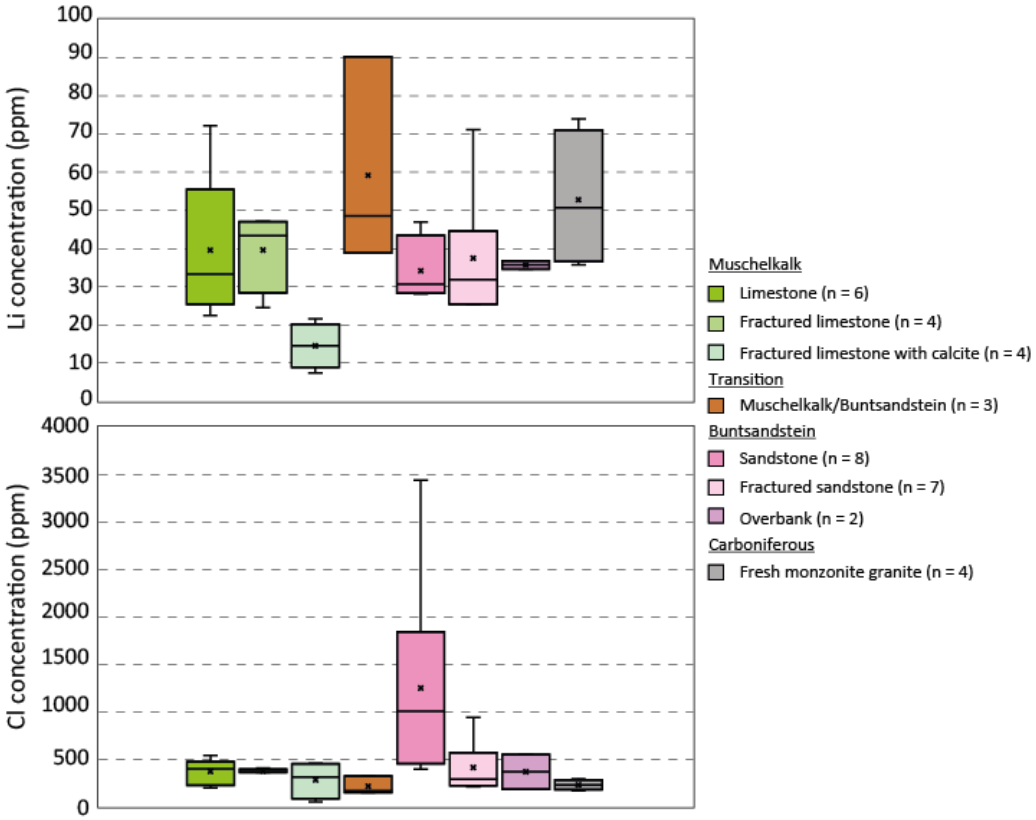


**Figure 6: These boxplot diagrams illustrate the distribution of [Li] and [Cl] in the Muschelkalk and Buntsandstein compared to the fresh monzonite granite studied in Fries et al., 2025. The box represents the interquartile range (IQR), encompassing the middle 50% of the data. The horizontal line within the boxes indicates the median concentration, and the cross indicates the average concentration. Whiskers extend to the smallest and largest values within 1.5 times the IQR from the lower and upper quartiles, respectively.**

### 4.2 [Li] and permeable zones at well scale

[Li] concentrations were plotted along depth in the various lithologies encountered in the Muschelkalk and the Buntsandstein for both EPS-1 and GPK-1 wells. The [Li] are correlated with static geophysical logs (gamma-ray, porosity) and dynamic well logs (temperature) as well as porosity and permeability measurements on core samples from the EPS-1 well (Figure 7).

At a large scale along depth, the [Li] values are more variable in the Muschelkalk compared to the Buntsandstein where [Li] values are more stable. In the Muschelkalk, the mean [Li] in the EPS-1 well is 35.5 ppm (n = 14) compared to 14.5 ppm (n = 2). The highest [Li] (90.2 ppm) is reached at the base of the Muschelkalk in the EPS-1 well and could be linked to a permeable fracture zone at FZ980. In the Buntsandstein, the mean [Li] in EPS-1 well is 35.4 ppm (n = 21) compared to 30 ppm (n = 4) in the GPK-1 well. The highest [Li] (71.1 ppm) in the Buntsandstein is reached in EPS-1 well in the GA. In the EPS-1 well, mostly in the Muschelkalk, the [Li] values seem to vary according to the gamma-ray (GR). The GR could react (measurement in K concentration) to an enrichment of clay minerals, thus suggesting that [Li] is correlated with clay content. This recurrent behaviour is visible on both EPS-1 and GPK-1 wells (Figure 7). The GR values increase and decrease along depth at the transition between the Muschelkalk and the Buntsandstein observed in EPS-1 and GPK-1. It is also visible in the close geothermal Rittershoffen wells (Glaas et al., 2025). This increase of the GR is surely underlying an increase in clay content at this lithostratigraphic transition, revealing a mineralogical composition mostly linked to the sedimentary composition rather than to fracture-controlled secondary depositions.

Furthermore, at this large scale, 3 main zones seem to be more porous and permeable after the core measurements data visible in the EPS-1 well (Figure 7). The particularity of these 3 zones is that they are recurrently located in the lower part of the 3 formations

of the Upper, Middle and Lower GV (PZ1130, PZ1230, PZ1330, Figure 7). These zones will be detailed hereafter.

At a more local scale along depth, several major permeable zones could be identified. In the further description, we will distinguish the permeability due to fracture zones (FZ) and porous zones (PZ) and link their occurrence with temperature anomalies and [Li] in both wells.

- EPS-1 well

**FZ950:** This zone presents a GR peak associated to a temperature anomaly visible on the thermal gradient revealing a permeable zone with secondary clay minerals precipitation. These peaks being very localized and sharp seem to be rather associated to the occurrence of a permeable fracture zone than to a matrix-controlled porous zone. To support this hypothesis, this permeable zone does not exist in the same lithology in the GPK-1 well and thus does not seem to be controlled to a porosity due to formation matrix. A marked increase of the [Li] is observed in this zone up to 72.2 ppm at 960 m which could be linked to secondary clay minerals deposition due to hydrothermal circulations. This zone is also characterized by the occurrence of hydraulic breccias at 942 and 962 m (Aichholzer et al., 2019).

**FZ980:** This zone has a similar response than the FZ950. A temperature anomaly is traduced by sharp peaks visible on the thermal gradient, but on the contrary no sharp peak is visible on the GR. This suggests the occurrence of a permeable fracture channelizing brine from the formation to the well. A marked increase of the [Li] is observed in this zone up to 90.2 ppm at 1000 m which could also be linked to secondary clay minerals deposition due to hydrothermal circulations.

**PZ1130, 1230 & 1330:** In these zones, no temperature anomaly is noticeable, even on the thermal gradient. However, these 3 zones present high porosity and permeability values measured on core samples, which are correlated with high porosities (NPHI) measured in the well. These 3 zones seem to reflect formation-matrix related porosity allowing high permeabilities which are not visible on the temperature log as they are producing a continuous impact on the thermal gradient. It is hard to correlate the occurrence of these 3 zones in the GPK-1 well, unless for the lowest part of the LGV corresponding to PZ1280 in GPK-1 (Figure 7). In these zones, [Li] does not seem to be affected by permeability and follows the mean values.

**FZ1200:** This zone presents a temperature anomaly visible on the thermal gradient, which is not correlated with GR peaks or even porosity log (NPHI), neither porosity and permeability measured on cores which are both quite low. Thus, the permeability of this zone seems more linked to a permeable fracture channelizing the flow from the formation to the wells. Hence, at 1200 m a major fault has been detected crossing the wells of SsF (Sausse et al., 2010). Several [Li] measurements have been done around this depth and some show slightly higher values (44 ppm) than the mean [Li] in the Buntsandstein (35 ppm).

- GPK-1 well

**FZ1000:** This zone is marked by a thermal gradient increase, a GR peak and neutron porosity (NPHI) peaks. No [Li] has been acquired at this depth. These responses seem to be linked to the occurrence of a permeable fracture channelizing the flow.

**FZ1200:** This zone is marked by GR peaks and neutron porosity peaks (NPHI) but no temperature anomaly is visible. This zone could correspond to the one seen in the EPS-1 well at the same depth, which could be due to the occurrence of a permeable fracture channelizing the flow from the formation to the wells. Hence, at 1200 m a major fault has been detected crossing the wells of SsF (Sausse et al., 2010). Several [Li] measurements have been done around this depth and some show slightly higher values (35 ppm) than the mean [Li] in the Buntsandstein (30 ppm).

**PZ1280:** In this zone, no temperature anomaly is identifiable, even on the thermal gradient. However, a high neutron porosity (NPHI) is measured. This zone could be permeable due to formation-matrix porosity related as in the EPS-1 well in the lowest part of the LGV PZ1330 (Figure 7). No [Li] has been acquired at this depth.

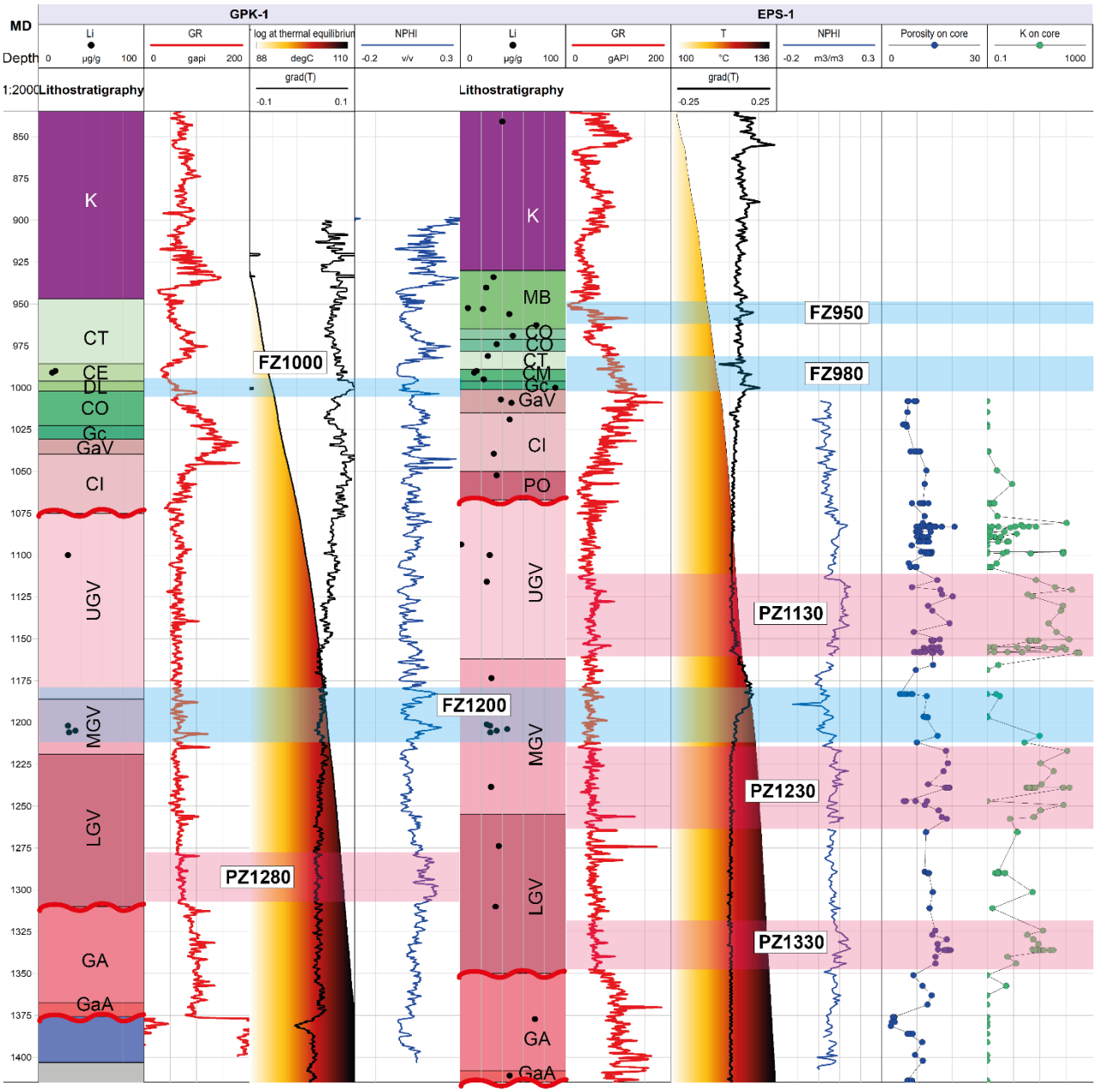


**Figure 7: Composite log showing the lithium values in depth in the wells EPS-1 and GPK-1, the lithostratigraphy (CC: Couches à Cératites, CE: Calcaire à Entroques, DL: Dolomie à Lingules, MB: Marnes Bariolées, CO: Dolomies & Calcaires Ondulés & Couches à Myacites, CT: Calcaire à Térabratules, GC: Grès Coquiller, GaV: Grès à Voltzia, CI: Couches Intermédiaires, U-M-LGV: Upper-Middle-Lower Grès Vosgien, GA: Grès d'Annweiler, GaA: Grès anté-Annweiler) according to Aichholzer et al., (2019, 2016), and static geophysical logs (gamma-ray, porosity), dynamic well logs (temperature) as well as porosity and permeability measurements on core samples for the EPS-1 well from Goupil et al., (2022); Griffiths et al., (2016); Heap et al., (2017).**

## 5. DISCUSSION

In the Buntsandstein, the Li concentrations measured in this study can be compared to the ones in cuttings samples collected in Permo-Triassic sedimentary rocks from 1750 to 1924 m depth in the well GB1 at Bruchsal ranging from 18 to 87 ppm (Figure 1; Kölbel et al., 2023). Additionally, in the North German Basin, Regenspurg et al., (2016) have measured [Li] comprised between 7 to 76 ppm ([Li] median = 14 ppm) in cuttings from the Permian formation (Rotliegend). In these clastic rock's cuttings, the authors highlighted that an increasing clay mineral content is accompanied by an increase in [Li]. Even if the lithostratigraphy is not strictly the same in both studies (Permian vs. Triassic) a similar observation showed that [Li] is correlated with GR values, and thus clay content.

In both the GPK-1 and EPS-1 wells, an increase in lithium concentration ([Li]) correlates with higher clay content. This trend appears to be primarily associated

with the presence of permeable fracture zones rather than with matrix porosity. This could suggest higher fluid-rock interactions through fractures than through porosity. However, Li could be also depleted from the rock by brine circulating in porosity or in fractures and only localized specific conditions related to permeable fractures could enable to precipitate higher [Li]. This hypothesis aligns with findings from Variscan crystalline rocks in the same wells, where lithium concentrations reach up to 156 ppm in localized granite veins or fracture fillings containing secondary quartz and illite (Fries et al., 2025). The same process could occur in the Buntsandstein and in the Muschelkalk but with significantly lower concentrations: up to 90 ppm in the Muschelkalk and 70 ppm in the Buntsandstein.

The median [Cl] in the analyzed unfractured sandstones is 1005 ppm, which represents the highest chlorine levels recorded among all sampled lithologies, including granite (Fries et al., 2025). This elevated [Cl] content in unfractured sandstones suggests that chlorine is likely retained in the rock matrix, possibly in the form of fluid inclusions or soluble salts. Thus, the absence of natural fractures may limit fluid circulation which is coherent with the previous hypothesis. The significantly higher [Cl] values in the unfractured sandstone compared to both fractured sandstones and other lithologies (e.g. granite) highlight the importance of structural features in controlling [Cl] and also [Li].

## 6. CONCLUSION

First geochemical analyses of lithium concentrations in the Triassic rocks from the Upper Rhine Graben have been presented. Lithium concentrations in these sedimentary rocks are rather scattered in the Muschelkalk limestone formation but more stable in the Buntsandstein clastic formation. However, lithium concentrations in the Triassic formations are significantly lower than those observed in the deep-seated Variscan granitic rocks. Future studies will aim to correlate lithium concentrations with fracture characteristics (e.g., density and aperture) to better understand the relationship between permeability and structural occurrence. Also X-Ray diffraction data will help to identify precisely the minerals releasing Li, and isotopic Li analyses will be realized on the rock and on the brine, which could help to identify the rock origin of the [Li] in the brine.

## REFERENCES

Aichholzer, C., Duringer, Ph., Genter, A., 2019. Detailed descriptions of the lower-middle Triassic and Permian formations using cores and gamma-rays from the EPS-1 exploration geothermal borehole (Soultz-sous-Forêts, Upper Rhine Graben, France). Geotherm. Energy 7, 34. https://doi.org/10.1186/s40517-019-0148-1

Aichholzer, C., Duringer, Ph., Orciani, S., Genter, A., 2016. New stratigraphic interpretation of the Soultz-sous-Forêts 30-year-old geothermal wells calibrated on the recent one from Rittershoffen (Upper Rhine Graben, France). Geotherm. Energy 4, 13. https://doi.org/10.1186/s40517-016-0055-7

Baujard, C., Genter, A., Dalmais, E., Maurer, V., Hehn, R., Rosillette, R., Vidal, J., Schmittbuhl, J., 2017. Hydrothermal characterization of wells GRT-1 and GRT-2 in Rittershoffen, France: Implications on the understanding of natural flow systems in the Rhine graben. Geothermics 65, 255–268. https://doi.org/10.1016/j.geothermics.2016.11.001

Bofill, L., Bozetti, G., Schäfer, G., Ghienne, J.-F., Schuster, M., Heap, M., Knobelock, G., Scherer, C., Armenlenti, G., de Souza, E., 2025. Sedimentary control on permeability heterogeneity: the Middle Buntsandstein continental sandstones (Lower Triassic, eastern France). Mar. Pet. Geol. 173. https://doi.org/10.1016/j.marpetgeo.2024.107261

Bosia, C., Mouchot, J., Ravier, G., Seibt, A., Jähnichen, S., Degering, D., Scheiber, J., Baujard, C., Genter, A., 2021. Evolution of brine geochemical composition during operation of EGS geothermal plants (Alsace, France), in: Proceedings, 46th Workshop on Geothermal Reservoir Engineering. Presented at the 46th Workshop on Geothermal Reservoir Engineering, Stanford University, Stanford, California, p. 21.

Fries, D., Glaas, C., Genter, A., 2025. Hydrothermal alteration role on lithium mobility in a geothermal reservoir: Geochemical analyses of deep granite in the Upper Rhine Graben, in: Proceedings, 50th Workshop on Geothermal Reservoir Engineering Stanford University. Presented at the 50th Workshop on Geothermal Reservoir Engineering Stanford University, Stanford University, California, USA.

Genter, A., Evans, K., Cuenot, N., Fritsch, D., Sanjuan, B., 2010. Contribution of the exploration of deep crystalline fractured reservoir of Soultz to the knowledge of enhanced geothermal systems (EGS). Comptes Rendus Geosci., Vers l'exploitation des ressources géothermiques profondes des systèmes hydrothermaux convectifs en milieux naturellement fracturés 342, 502–516. https://doi.org/10.1016/j.crte.2010.01.006

Glaas, C., Salmon, M., Baron, F., Bozetti, G., Knobelock, G., Rumbach, G., Patrier, P., Baczkowski, C., Gentera, A., 2025. Are Triassic rocks of the Upper Rhine Graben a geothermal reservoir? Insights from Rittershoffen wells with geophysical logs and SWIR spectroscopy. Presented at the European Geothermal Congress, Zürich, Switzerland.

Goupil, M., Heap, M.J., Baud, P., 2022. Permeability anisotropy in sandstones from the Soultz-sous-Forêts geothermal reservoir (France):

implications for large-scale fluid flow modelling. Geotherm. Energy 10, 32. https://doi.org/10.1186/s40517-022-00243-1

Griffiths, L., Heap, M.J., Wang, F., Daval, D., Gilg, H.A., Baud, P., Schmittbuhl, J., Genter, A., 2016. Geothermal implications for fracture-filling hydrothermal precipitation. Geothermics 64, 235–245. https://doi.org/10.1016/j.geothermics.2016.06.006

Heap, M.J., Kushnir, A.R.L., Gilg, H.A., Wadsworth, F.B., Reuschlé, T., Baud, P., 2017. Microstructural and petrophysical properties of the Permo-Triassic sandstones (Buntsandstein) from the Soultz-sous-Forêts geothermal site (France). Geotherm. Energy Heidelb. 5, 1–37. https://doi.org/10.1186/s40517-017-0085-9

Horstman, E.L., 1957. The distribution of lithium, rubidium and caesium in igneous and sedimentary rocks. Geochim. Cosmochim. Acta 12, 1–28. https://doi.org/10.1016/0016-7037(57)90014-5

Johns, W.D., Huang, W.H., 1967. Distribution of chlorine in terrestrial rocks. Geochim. Cosmochim. Acta 31, 35–49. https://doi.org/10.1016/0016-7037(67)90096-8

Kölbel, L., Ghergut, I., Sauter, M., Kölbel, T., Wiegand, B., 2021. Integrated approach into the characterization of the fracture network of a geothermal reservoir. Appl. Geochem. 129, 104967. https://doi.org/10.1016/j.apgeochem.2021.104967

Kölbel, L., Kölbel, T., Herrmann, L., Kaymakci, E., Ghergut, I., Poirel, A., Schneider, J., 2023. Lithium extraction from geothermal brines in the Upper Rhine Graben: A case study of potential and current state of the art. Hydrometallurgy 221, 106131. https://doi.org/10.1016/j.hydromet.2023.106131

Ogita, H., Nakai, N., Oana, S., 1967. Chlorine in sedimentary rocks. Geochem. J. 1, 139–148. https://doi.org/10.2343/geochemj.1.139

Ravier, G., Fries, D., Seibel, O., Ólafsson, D.I., Ledésert, B., 2022. Investigations on brine transport pipes for upscaling geothermal plants in the Upper Rhine Graben, in: European Geothermal Congress. Presented at the European Geothermal Congress 2022, Berlin, Germany.

Regenspurg, S., Feldbusch, E., Norden, B., Tichomirowa, M., 2016. Fluid-rock interactions in a geothermal Rotliegend/Permo-Carboniferous reservoir (north German basin). Appl. Geochem. 69, 12–27.

Sanjuan, B., Millot, R., Innocent, Ch., Dezayes, Ch., Scheiber, J., Brach, M., 2016. Major geochemical characteristics of geothermal brines from the Upper Rhine Graben granitic basement with constraints on temperature and circulation. Chem. Geol. 428, 27–47. https://doi.org/10.1016/j.chemgeo.2016.02.021

Sausse, J., Dezayes, C., Dorbath, L., Genter, A., Place, J., 2010. 3D model of fracture zones at Soultz-sous-Forêts based on geological data, image logs, induced microseismicity and vertical seismic profiles. Comptes Rendus Geosci. 342, 531–545. https://doi.org/10.1016/j.crte.2010.01.011

Vernoux, J.F., Genter, A., Razin, P., Vinchon, C., 1995. Geological and petrophysical parameters of a deep fractured sandstone formation as applied to geothermal exploitation (public No. R 38622). BRGM Orléans, France.

Weynell, M., Wiechert, U., Schuessler, J.A., 2017. Lithium isotopes and implications on chemical weathering in the catchment of Lake Donggi Cona, northeastern Tibetan Plateau. Geochim. Cosmochim. Acta 213, 155–177.

Stanford, California, USA, (2021), 16-18 February 2021.

Duringer, Ph., Orciani, S., Aichholzer, C., and Genter, A.: The complete lithostratigraphic section of the geothermal wells in Rittershoffen (Upper Rhine Graben, eastern France): a key for future geothermal wells, *Bulletin Société Géologique de France*, **190**, (2019), 13.

Fries, D., Glaas, C., and Genter, A.: Hydrothermal alteration role on lithium mobility in a geothermal reservoir: geochemical analyses of deep granite in the Upper Rhine Graben. *Proceedings of the Stanford Geothermal Workshop 2025*, Stanford, California, USA, (2025), 10-12 February 2025.

Genter, A., Evans, K.F., Cuenot, N., Fritsch, D., and Sanjuan, B.: Contribution of the exploration of deep crystalline fractured reservoir of Soultz to the knowledge of Enhanced Geothermal Systems (EGS). *Comptes Rendus Geoscience*, **342**, (2010), 502-516.

Kölbel, L., Ghergut, J., Sauter, M., Kölbel, Th., and Wiegand, B.: Integrated approach into the characterization of the fracture network of a geothermal reservoir, *Applied Geochemistry*, **129**, (2021), 104967, ISSN 0883-2927,

Sanjuan, B., Millot, R., Innocent, Ch., Dezayes, Ch., Scheiber, J. and Brach, M.: Major geochemical characteristics of geothermal brines from the Upper Rhine Graben granitic basement with constraints on temperature and circulation. *Chemical Geology*. **428**, (2016), 27-47.

Vernoux, J.F, Genter, A., Razin, P., and Vinchon, C.: Geological and petrophysical parameters of a deep fractured sandstone formation as applied to geothermal exploitation, EPS-1 borehole, Soultz-sous-Forêts, France, *BRGM Open File Report*, **R 38622**, 69 pp.

Vidal, J., and Genter, A.: Overview of naturally permeable fractured reservoirs in the central and southern Upper Rhine Graben: insights from geothermal wells. *Geothermics*, **74**, (2018), 57-73.

**Acknowledgements**

This project research, LICORNE was funded by the European Union under Grant Agreement No 101069644. Views and opinions expressed are however those of the authors only and do not necessarily reflect those of the European Union or the European Climate, Infrastructure and Environment Executive Agency (CINEA). Neither the European Union nor the granting authority can be held responsible for them. The authors are grateful to GEIE Exploitation Minière de la Chaleur for accessing the cores at the Soultz-sous-Forêts geothermal site.